

Article

Verification of MPACT for the APR1400 Benchmark

Kaitlyn Elizabeth Barr ^{1,*} , Sooyoung Choi ¹ , Junsu Kang ²  and Brendan Kochunas ¹ 

¹ Department of Nuclear Engineering and Radiological Sciences, University of Michigan, Ann Arbor, MI 48109, USA; sooychoi@umich.edu (S.C.); bkochuna@umich.edu (B.K.)

² Department of Nuclear Engineering, Seoul National University, Seoul 08826, Korea; js0826@snu.ac.kr

* Correspondence: bkaitlyn@umich.edu

Abstract: This paper describes benchmark calculations for the APR1400 nuclear reactor performed using the high-fidelity deterministic whole-core simulator MPACT compared to reference solutions generated by the Monte Carlo code McCARD. The methodology presented in this paper is a common approach in the field of nuclear reactor analysis, when measured data are not available for comparison, and may be more broadly applied in other simulation applications of energy systems. The benchmark consists of several problems that span the complexity of single pins to a hot full power cycle depletion. Overall, MPACT shows excellent agreement compared to the reference solutions. MPACT effectively predicts the reactivity for different geometries and several temperature and boron conditions. The largest deviation from McCARD occurs for cold zero conditions in which the fuel, moderator, and cladding are all 300 K. Possible reasons for this are discussed. Excluding these cases, the ρ reactivity difference from McCARD is consistently below 100 pcm. For single fuel pin problems, the highest error of 151 pcm occurs for the lowest fuel enrichment of 1.71 wt.% UO₂, indicating possible, albeit small, enrichment bias in MPACT's cross-section library. Furthermore, MOC and spatial mesh parametric studies indicate that default meshing parameters and options yield results comparable to finely meshed cases. Additionally, there is very good agreement of the radial and axial power distributions. RMS radial pin and assembly power differences for all cases are at or below 0.75%, and all RMS axial power differences are below 1.65%. These results are comparable to previous results from the VERA progression problems benchmark and meet generally accepted accuracy criteria for whole-core transport codes.

Keywords: MPACT; VERA-CS; APR1400; benchmark



Citation: Barr, K.E.; Choi, S.; Kang, J.; Kochunas, B. Verification of MPACT for the APR1400 Benchmark. *Energies* **2021**, *14*, 3831. <https://doi.org/10.3390/en14133831>

Academic Editors: Arturo Buscarino and Ricardo J. Bessa

Received: 6 May 2021

Accepted: 19 June 2021

Published: 25 June 2021

Publisher's Note: MDPI stays neutral with regard to jurisdictional claims in published maps and institutional affiliations.



Copyright: © 2021 by the authors. Licensee MDPI, Basel, Switzerland. This article is an open access article distributed under the terms and conditions of the Creative Commons Attribution (CC BY) license (<https://creativecommons.org/licenses/by/4.0/>).

1. Introduction

The whole-core neutron transport calculation is becoming a more attractive simulation paradigm for reactor physics due to the significant advancements in high-performance computing over the last decade. The pin-resolved neutron transport calculation can improve overall solution accuracy by eliminating numerous approximations used in the commercial two-step lattice transport/nodal diffusion calculation procedure. It is expected that the direct whole-core transport calculation can enhance the accuracy of reactor design parameters and safety margin. Moreover, it is possible to provide more detailed information, such as intra-pin level solutions that cannot be calculated by conventional reactor design tools. Due to these advantages, many codes based on the whole-core transport calculation were developed in last decade. Although these tools can provide higher-fidelity solutions that are arguably more accurate than the conventional reactor design tools, this comes with a significant increase in computing costs. The whole-core neutron transport calculation will never replace the conventional design tools, but it can serve an important role for the verification of the conventional tools and be useful in some very specific applications.

However, before the benefits of state-of-the-art modeling and simulation of nuclear reactors can be realized for designing new reactors, some level of validation is needed to establish confidence in the tools capability to design something that has never been built.

Generally, in the reactor analysis field, validation implies comparison with measured data. This conundrum of needing to validate design tools for designs that have no measured data are a frequent occurrence for reactor physicists. The field overall has developed an approach that is commonplace to compare the design tools to extremely high-fidelity reference solutions where the methodology may be considered to be the “gold standard” for the field and make use of practically no approximations. In the computational reactor physics community these types of comparisons are often considered to be good as validation—albeit different. For researchers new to this field, this perspective sometimes seems a bit unconventional and even erroneous. To address this misconception, and broaden the understanding of general methods used by reactor physicist, we provide a detailed example of this type of activity in this paper that is widely accepted by the reactor physics community. For the broad readership of this journal, we hope that this manuscript help to improve the acceptance of ultra-high-fidelity reference solutions as a means of the best validation available.

Compared to the traditional two-step procedure, whole-core simulators are still in a phase of maturity where verification and validation are critical activities to establish the credibility of these codes and their methods. Furthermore, the verification and validation of the transport codes are necessary for the application of high-fidelity tools in the production calculations. Comparison of simulation to experiment to establish validation is the gold standard. MPACT and VERA have been extensively validated [1–3], and only recently has the validation of high-fidelity deterministic transport codes for the calculation of intra-pin reaction rate distributions been established [4]. However, in many cases, high quality validation data may not be available for a variety of reasons. This circumstance is particularly relevant when considering the analysis of advanced reactors where operational data does not yet exist. Consequently, when applying high-fidelity simulators to new reactors, something other than comparison to measured data is needed. In this case, code-to-code verification is often the best thing that can be done. The transport solution from the whole-core transport code is most often verified against the Monte Carlo solution, since it uses less approximation than the deterministic transport code in terms of energy representation. Still, verification against Monte Carlo can be impractical or suspect when considering the operational cycle. Thus, code-to-code comparison of high-fidelity deterministic simulation tools is a central activity to furthering their improvements and establishing their credibility.

In this paper, we present comparisons of several leading high-fidelity simulators to each other and reference Monte Carlo results for the APR1400 reactor that were performed as a part of an I-NERI collaboration.

I-NERI is a joint venture between the United States and the Republic of Korea that aims to address pressing challenges to nuclear power [5]. In a 2019 I-NERI program, the APR1400 benchmark, based on the core design of the Korea Electric Power Corporation Advanced Power Reactor 1400 MWe (APR1400), was developed to facilitate code-to-code verification of high-fidelity, multi-physics simulation codes for advanced nuclear reactors [6]. The benchmark reference solution was generated by the Monte Carlo code McCARD [7]. Hence, the purpose of this paper is to describe and present the results of a series of benchmark calculations performed using the Michigan PARallel Characteristics Transport (MPACT) code [8] and discuss the extent of agreement with the McCARD reference solution. McCARD was used to provide reference results instead of measured data because measurements have not been made available for this benchmark. The benchmark problems were completed using MPACT because it offers some advantages for detailed calculations when compared to McCARD. Specifically, Monte Carlo codes such as McCARD generally provide more accurate results due to the use of continuous energy cross-sections while deterministic codes apply the multigroup approximation. However, for large problems such as a whole-core calculation or performing cycle depletion calculations, it is very computationally expensive for Monte Carlo codes to determine the pin power distribution and isotopics with small statistical errors. Thus, for detailed analysis of larger problems requiring knowledge of pin power distributions and very accurate isotopics, MPACT can

complete the same problem with fewer computational resources than a Monte Carlo code such as McCARD.

The analysis of these benchmark problems has also been completed by researchers by the Seoul National University Reactor Physics Laboratory using nTRACER and by KAERI using the Deterministic Core Analysis based on Ray Tracing (DeCART) code. DeCART is a “whole-core neutron transport code capable of direct subpin level flux calculation at power generating conditions” [9]. nTRACER is a “high-fidelity multi-physics simulation code” for commercial PWRs and fast reactors that uses a “direct whole-core calculation module and a sub-channel thermal/hydraulic solver” [10]. Both DeCART and nTRACER accurately predict reactivity in various geometries and conditions, with ρ reactivity differences from McCARD below 100 pcm in almost every case and control rod worth differences below 1.0%. For both codes, the greatest reactivity differences occur for cold zero conditions in which the fuel, moderator, and cladding are 300 K. These results are similar to those obtained using MPACT.

Regarding the power distribution, nTRACER results initially exhibited a radial power tilt, and this was resolved by correcting the reflector cross-sections for the large spatial dependency of the multigroup cross-sections for stainless steel. Once this was done, RMS radial power distribution errors between nTRACER and McCARD were all below 1.0% and RMS axial power distribution errors were below 1.7%. Radial power distribution errors were higher for DeCART; most RMS radial power distribution errors are below 1%, but there are several outliers, most of which are cases with cold zero power conditions. All RMS radial power distribution errors are below 2.27%. All RMS axial power differences from McCARD are below 2.25%. Excluding cases with cold zero conditions, all axial power differences are below 1.52% [11]. These results indicate that both DeCART and nTRACER effectively predict reactivity and power distributions for the APR1400, but errors are most significant for cases using cold zero conditions.

The remainder of this paper is outlined as follows. In Section 2, the reactor geometry, benchmark problems, and conditions studied are described in detail. In Section 3, all benchmark problem results as well as the results of spatial and MOC parametric mesh studies for single pin and 2-D single assembly cases are presented. In Section 4, modeling parameters used in the MPACT models as well as equations relevant for the analysis are included. Finally, Sections 5 and 6 contain conclusions and future work.

2. Benchmark Problems

The benchmark involves six problem types: a single fuel pin, single 2-D lattices, a 2-D core, a 3-D core, control rod worth calculations, and a 3-D core depletion. Additionally, mesh sensitivity studies were performed on the single fuel pin and single 2-D fuel assembly problems.

For each benchmark problem, several operating conditions are specified. For this report, cold zero (CZ) power refers to a moderator, cladding, and fuel temperature of 300 K. Hot zero (HZ) power indicates a moderator, cladding, and fuel temperature of 600 K. Hot full (HF) power refers to a moderator and cladding temperature of 600 K and a fuel temperature of 900 K. The specified boron concentrations are 0 ppm, 1000 ppm, and 2000 ppm. The naming convention adopted for describing the benchmark cases in this paper references cases using two letters that refer to the temperature condition, followed by a number that indicates the boron concentration. A boron concentration of 0 ppm is indicated by a 0, 1000 ppm is indicated by a 1, and 2000 ppm is indicated by a 2. For example, when the moderator, fuel, and cladding temperature are all 300 K and the boron concentration is 1000 ppm, the case is referred to as CZ1. Table 1 summarizes the naming conventions for all temperature and boron conditions that are analyzed.

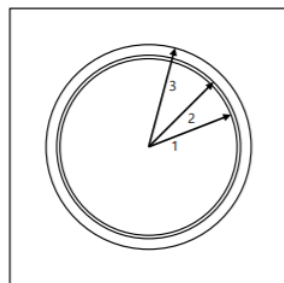
Table 1. Naming Convention for Various Temperature Conditions and Boron Concentrations.

Boron Concentration [ppm]	Temperature Conditions		
	CZP Fuel: 300 K Mod: 300 K	HZP Fuel: 600 K Mod: 600 K	HFP Fuel: 900 K Mod: 600 K
0	CZ0	HZ0	HF0
1000	CZ1	HZ1	HF1
2000	CZ2	HZ2	HF2

The APR1400 core consists of 241 fuel assemblies in a rectangular lattice. Each fuel assembly is composed of 236 fuel or burnable absorber rods, 4 guide tubes, and 1 central tube also arranged in a rectangular lattice.

Figures 1–4 show key elements of the APR1400 core configuration.

Figures 1 and 2 present radial and axial views of the fuel rods, respectively.



Region #	Size [cm]	Material
1	0.409575	UO2 Fuel
2	0.41873	AIR
3	0.47498	ZIRLO

Figure 1. Radial Configuration of Fuel Rod [6].

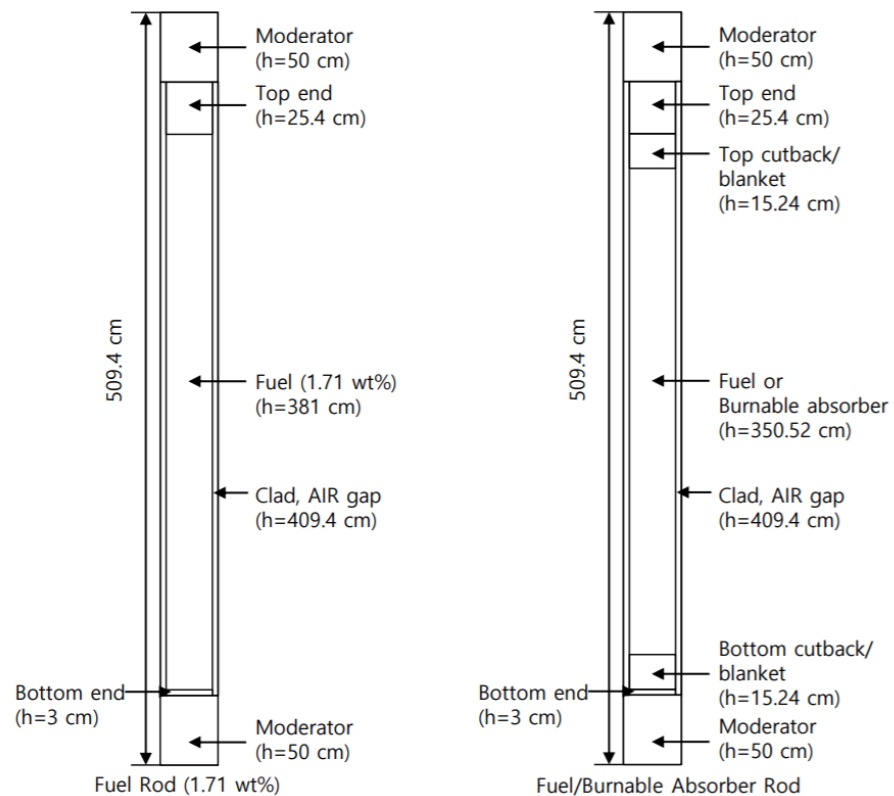


Figure 2. Axial Layout of Fuel and Burnable Absorber Rods in A0 Fuel Assembly (Left) and All Other Fuel Assemblies (Right) [6].

Figure 3 depicts the radial configuration of a fuel assembly and shows that all guide tubes and central tubes are the same size as four pin cells.

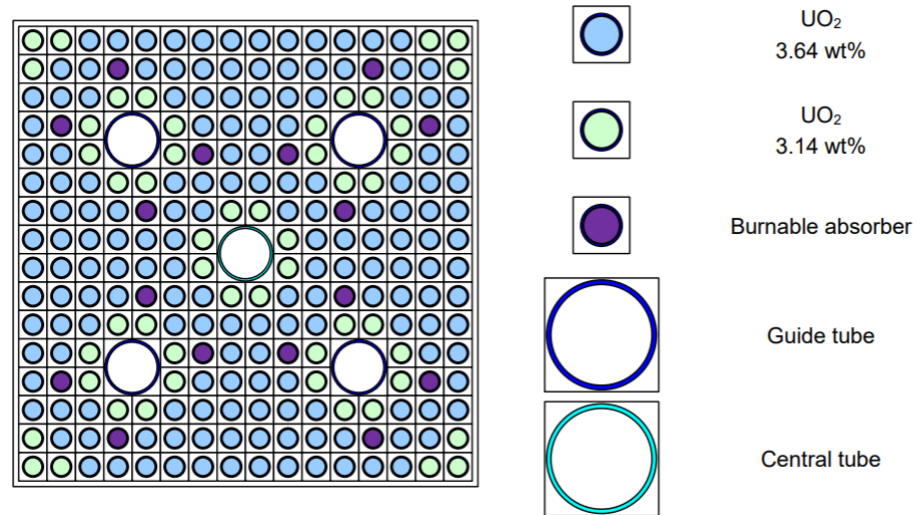


Figure 3. Radial Layout of C2 Fuel Assembly [6].

The core layout is shown in the left image in Figure 4. The reactor is controlled by seven control rod banks: five regulating banks, labeled 1, 2, 3, 4, and 5, and two shutdown banks, labeled A and B, as shown in the right image in Figure 4. Banks A, B, 1, and some of bank 2 are composed of 12-fingered control rod assemblies, and the rest of bank 2 as well as banks 3, 4, and 5 are composed of 4-fingered control rod assemblies.

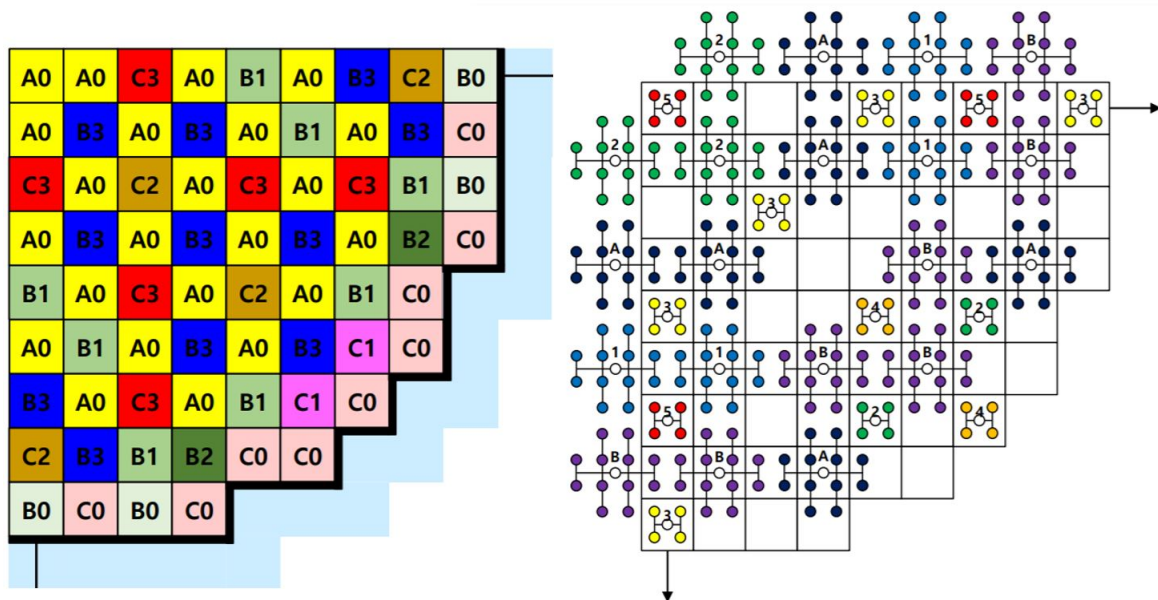


Figure 4. APR1400 Core Loading Pattern (left) and Control Rod Assembly Configuration (right) [6].

Figures 5–7 depict single fuel pin, single 2-D fuel assembly, and 2-D core problem geometries as modeled in MPACT. The light blue background represents water, light grey is cladding, purple is gadolinia burnable absorbers, and different fuel enrichments are represented by a spectrum ranging from dark blue, representing the lowest enrichment of 1.71 wt.% UO_2 , to maize, representing the highest enrichment of 3.64 wt.% UO_2 .

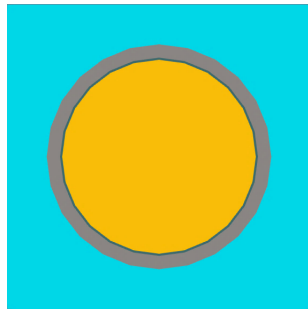


Figure 5. Single Fuel Pin Cell with 3.64 wt.% UO_2 as Modeled by MPACT.

There are nine different fuel assemblies: A0, B0, B1, B2, B3, C0, C1, C2, and C3. These use different configurations of 1.71 wt.% UO_2 , 2.64 wt.% UO_2 , 3.14 wt.% UO_2 , 3.64 wt.% UO_2 .

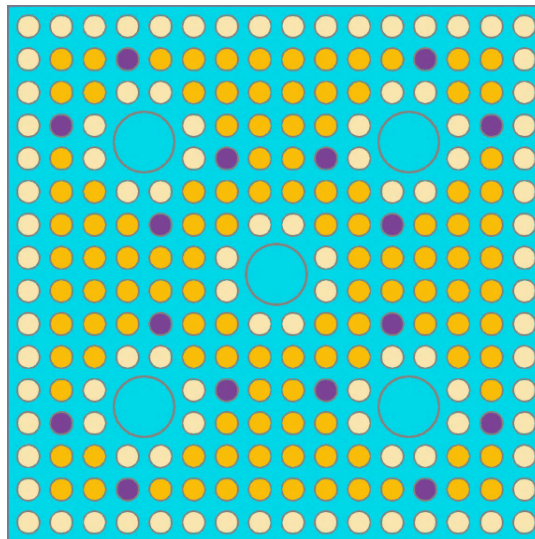


Figure 6. C3 Fuel Assembly Model Generated by MPACT.

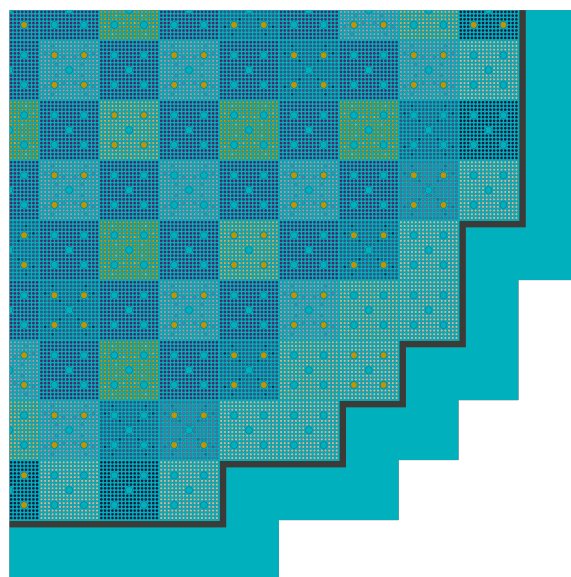


Figure 7. 2-D Core Model in MPACT.

3. Results and Discussion

3.1. Single Fuel Pin

3.1.1. Benchmark Problem Results

For the single pin problems, each of the five enrichments (1.71 wt.% UO₂, 2.00 wt.% UO₂, 2.64 wt.% UO₂, 3.14 wt.% UO₂, and 3.64 wt.% UO₂) was modeled for each of the nine temperature and boron conditions, for a total of 45 cases studied. The complete isotopic compositions of the fuel are specified in the benchmark and were manually defined in the inputs. Figure 8 is a histogram depicting the number of cases that fall in each reactivity difference range defined on the horizontal axis.

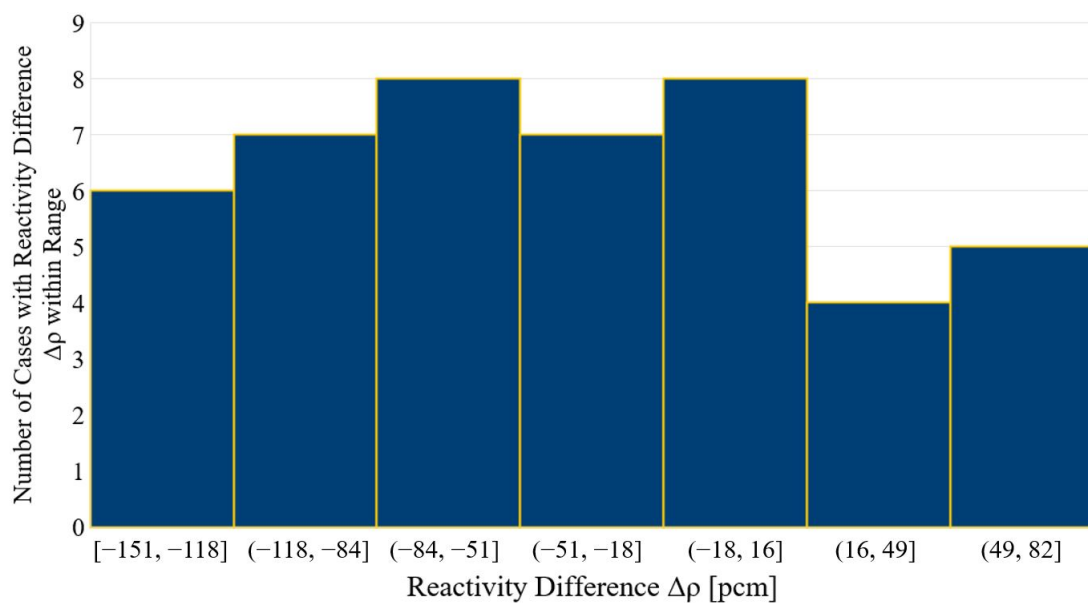


Figure 8. Histogram of Reactivity Differences for Single Fuel Pin Cases.

MPACT and McCARD generally agree very well; the average difference in k_{inf} between the two solutions was $63 \text{ pcm} \pm 44 \text{ pcm}$, which can be attributed to MPACT's usage of a multigroup approximation as opposed to McCARD's continuous energy cross-section representation. In 34 of the 45 cases studied, MPACT had a lower k_{inf} than McCARD, demonstrating a possible bias in the cross-section libraries. The maximum difference in k_{inf} was 151 pcm, and the minimum difference was 3 pcm.

Table 2 contains the average reactivity difference, standard deviation, and maximum reactivity difference for various categories of cases to better identify specific trends in the results. It was determined that the largest relative differences were observed for cases with an enrichment of 1.71 wt.% UO₂, suggesting a possible, slight enrichment bias of approximately -50 pcm , although the exact value depends on other conditions, e.g., temperature, moderator density, boron concentration, in MPACT's cross-section library. Additionally, boron concentration had a moderate impact on accuracy, as observed in Table 2, which shows agreement with McCARD generally improving as boron concentration increases.

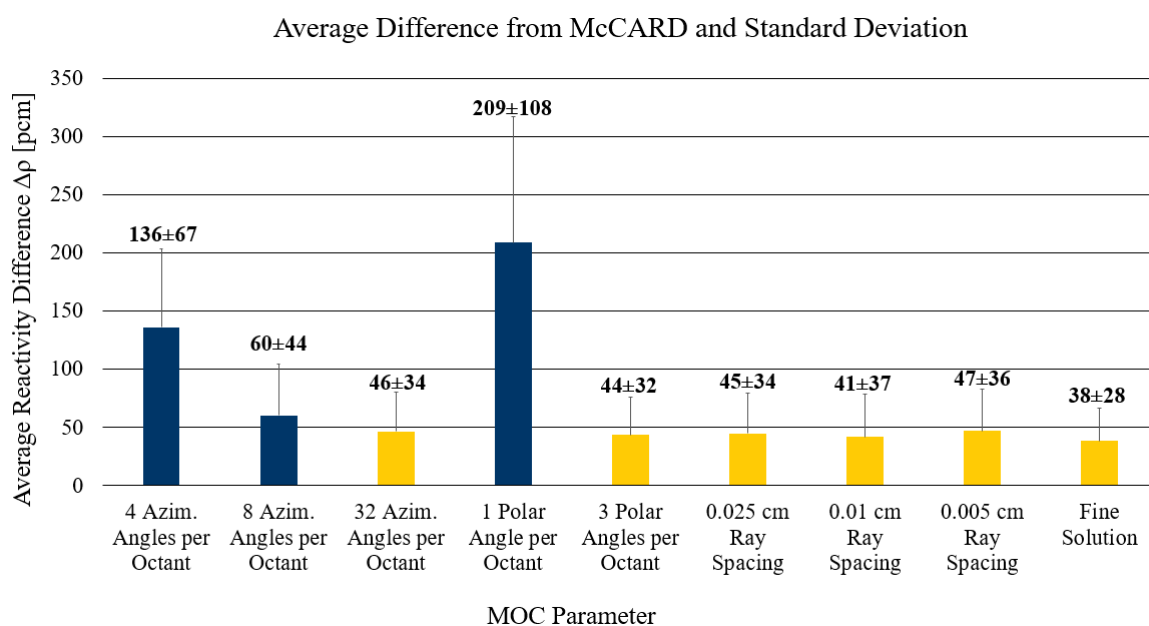
Table 2. Average reactivity difference, standard deviation, and maximum difference for various groups of single fuel pin cases.

Condition	Average $k_{inf} \Delta\rho$ [pcm]	Standard Deviation [pcm]	Maximum Difference [pcm]
Overall	63	44	151
0 ppm	110	22	151
1000 ppm	44	32	123
2000 ppm	28	35	82
1.71 wt.%	79	76	151
2.00 wt.%	66	73	134
2.64 wt.%	58	67	122
3.00 wt.%	53	61	116
3.64 wt.%	48	57	104
CZ	75	87	151
HZ	64	47	104
HF	60	49	138

Reference [12] outlines several accuracy goals, including that reactivity differences should be below 200 pcm. Given that the maximum reactivity difference from McCARD for pin cell cases is 151 pcm, these results are acceptable.

3.1.2. MOC Parametric Studies

MOC parameters were individually altered for each of the 3.64 wt.% enriched single pin cases, including all temperature and boron conditions, and compared to the k_{inf} generated by McCARD. Variations included using 4, 8, and 32 azimuthal angles per octant instead of the default 16; 1 and 3 polar angles per octant instead of the default 2; and 0.025 cm, 0.01 cm, and 0.005 cm ray spacing instead of the default 0.05 cm. Figure 9 summarizes the average differences between the k_{inf} generated using each of these parameters and the k_{inf} generated by McCARD.

**Figure 9.** Average difference from McCARD k_{inf} and standard deviation for single pin MOC studies.

In Figure 9, blue bars indicate parameters that are less fine than the default values, and maize bars indicate parameters that are finer than the default. Significant disagreement ranging from an average of 60 pcm to 209 pcm exists when parameters are made less

fine than the default. The maximum absolute difference from McCARD is 369 pcm. On the other hand, making the MOC parameters finer reduces the average ρ difference from McCARD with errors ranging from 38 pcm to 47 pcm. Since the average difference from McCARD for pins with 3.64 wt.% UO₂ using default values was 48 pcm, as stated in Table 2, there is a slight improvement in agreement with McCARD when using parameters finer than the default.

One of the parametric studies performed combined all the finest parameters and was called the “fine” solution. The fine solution had a ray spacing of 0.005 cm, 32 azimuthal angles per octant, and 3 polar angles per octant. The error from the McCARD k_{inf} for the fine solution is only 38 pcm, which is 10 pcm lower than the error when using default parameters. Figures 10 and 11 are histograms the number of cases that fall in each reactivity difference range defined on the horizontal axis for the fine solution (Figure 10) and when default parameters are used (Figure 11). The cases shown all have 3.64 wt.% UO₂ enrichment.

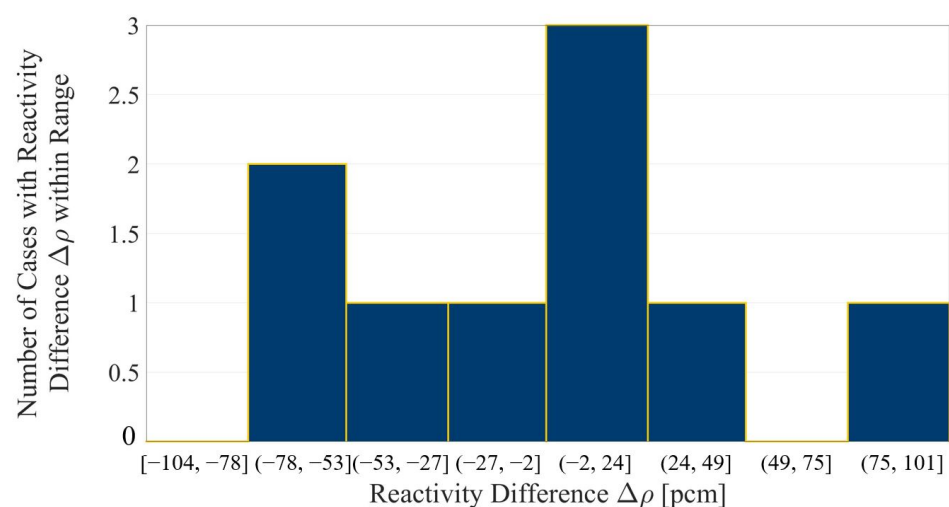


Figure 10. Histogram of reactivity differences for 3.64 wt.% UO₂ “fine” single fuel pin cases.

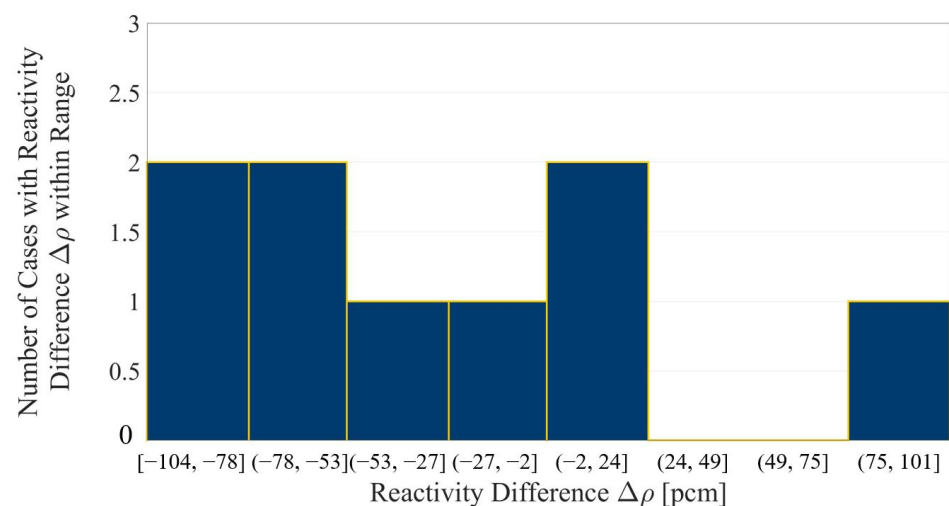


Figure 11. Histogram of reactivity differences for 3.64 wt.% UO₂ single fuel pin cases using default parameters.

In comparing the two figures, it is clear that most reactivities predicted by MPACT when using the fine parameters are lower than the reactivities reported by McCARD. Additionally, when using fine parameters, the reactivities are generally closer to the McCARD reference than when default parameters are used. However, the fine solution requires significantly more computational resources to compute; it takes three times as long and

uses almost four times as much memory. Given that the average reactivity agreement only improves by 10 pcm when using the finest parameters instead of default values and the tradeoff between accuracy and computational resources, the default parameters obtain suitable k_{inf} values.

3.1.3. Spatial Mesh Parametric Studies

For the spatial mesh studies, the number of radial subdivisions in the innermost region of the fuel cells was changed to be 1, 2, 4, or 5. For reference, the default solution has 3 subdivisions. The cases examined all had 3.64 wt.% UO_2 . When changing the mesh, ray spacing was set as 0.01 cm, and the azimuthal and polar angles per octant were left at the default values of 16 and 2, respectively. The average differences and standard deviation between the k_{inf} generated using 1, 2, 4, and 5 rings and the k_{inf} calculated by McCARD are shown in Figure 12.

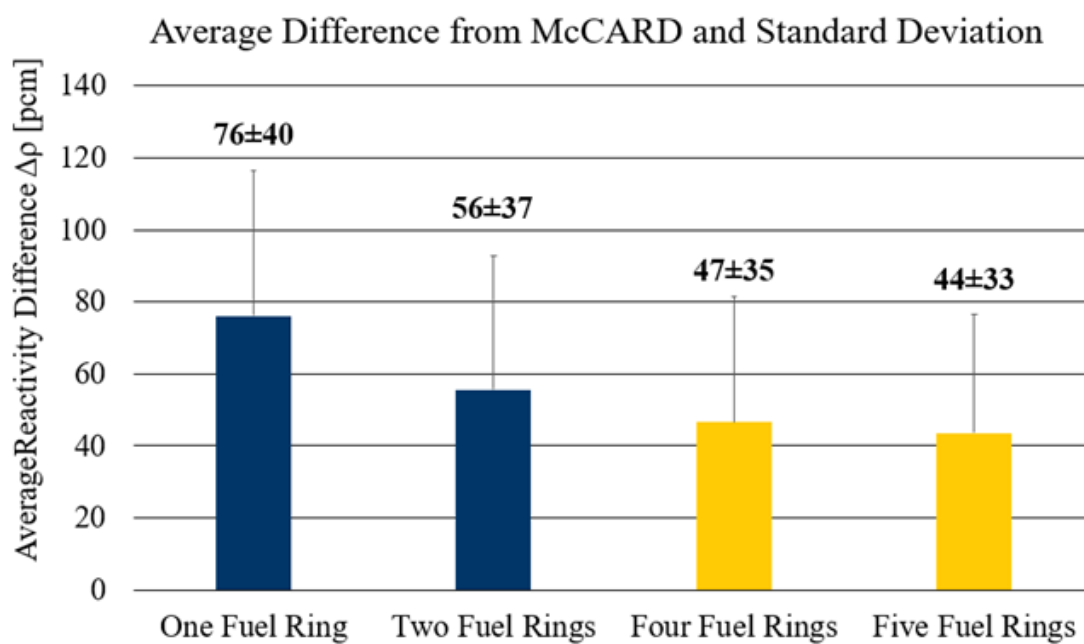


Figure 12. Average difference from McCARD k_{inf} and standard deviation for single pin spatial mesh studies.

In Figure 12, blue bars indicate parameters that are less fine than the default values, and maize bars indicate parameters that are finer than the default. Using coarser spatial meshes than the default results in reactivity differences from McCARD of 56 pcm for two fuel rings to 76 pcm for one fuel ring. A finer mesh results in reactivity differences from 47 pcm for four fuel rings to 44 pcm for five fuel rings. The reactivity differences for the finer meshes are only 1 pcm to 4 pcm below the reactivity difference of 48 pcm for the default mesh values. Considering that the finer cases take about 1.6 times longer and require about 1.4 times as much memory, and the minimum reactivity difference with McCARD is only 4 pcm lower than when default values are used, the default values are appropriate. Furthermore, altering the MOC parameters has a more significant impact on accuracy than altering the mesh of the problem.

3.1.4. Moderator Mesh Parametric Studies

For the moderator mesh studies, the number of radial subdivisions in the moderator was changed to be 2, 3, 4, or 5. For reference, the default solution has 1 subdivision. The cases examined all had 3.64 wt.% UO_2 . When changing the mesh, ray spacing was set to a fine spacing of 0.005 cm, and the azimuthal and polar angles per octant were set at 32 and 3, respectively. Additionally, the number of fuel rings increased to 5 from the default of 3.

The average differences and standard deviation between the k_{inf} generated using 2, 3, 4, and 5 rings and the k_{inf} calculated by McCARD are shown in Figure 13.

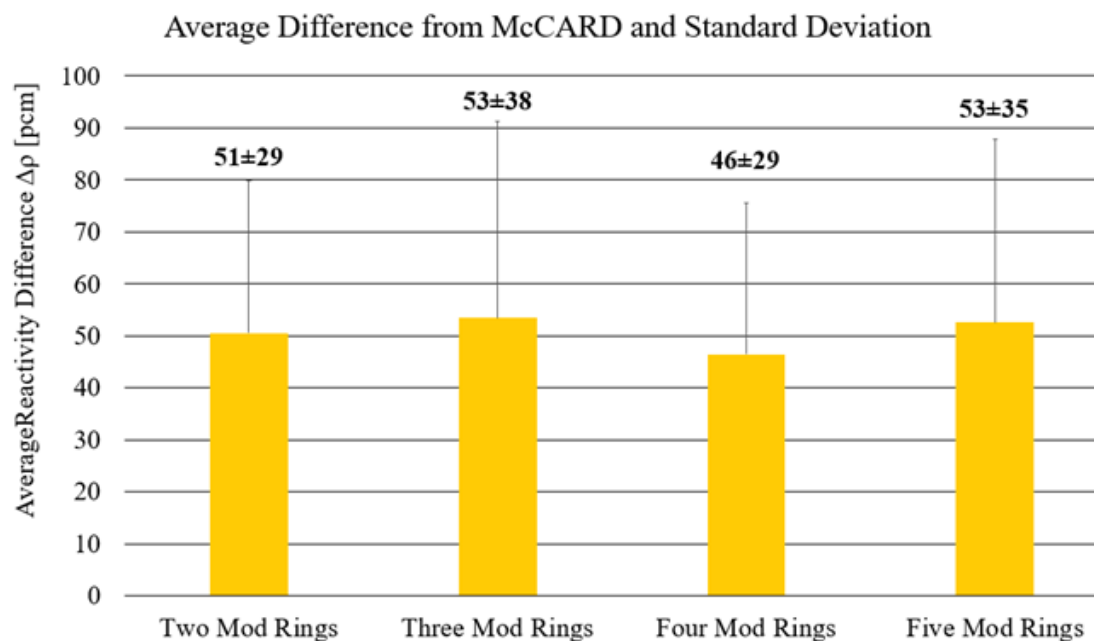


Figure 13. Average difference from McCARD k_{inf} and standard deviation for single pin moderator mesh studies.

When using the default value of one moderator ring, the average reactivity difference between MPACT and McCARD for 3.64 wt.% pins is 48 pcm. As Figure 13 shows, making the mesh finer causes agreement with McCARD to worsen in every case except for four moderator rings. Moreover, the finest moderator mesh of five rings has an average reactivity difference from McCARD of 53 pcm, which is 5 pcm higher than when using default values. Since, as noted earlier, when using the fine mesh, computation time is increased three-fold and memory usage is increased four-fold, it was determined that the default value of one moderator ring is most appropriate for use in generating benchmark results.

3.2. Single 2-D Assembly

3.2.1. Benchmark Problem Results

Each of the nine assembly types (A0, B0, B1, B2, B3, C0, C1, C2, C3) was run using all nine temperature and boron conditions. Figure 14 is a histogram that shows the number of cases falling each reactivity difference range defined on the horizontal axis.

The average difference from the McCARD k_{inf} values was $99 \text{ pcm} \pm 62 \text{ pcm}$, which again can be explained by MPACT using the multigroup approximation for its cross-sections. Unlike in the single pin problems, no significant biases in the cross-section libraries resulted in over- or under-predicting; MPACT overestimated k_{inf} in approximately half of the cases and underestimated in the rest compared to McCARD.

The pin powers within the assemblies generated by MPACT are very similar to the McCARD reference solutions, with an overall average RMS pin power difference of 0.22%. Given that a %RMS under 1% is usually satisfactory, the low %RMS difference suggests that MPACT's pin-resolved solution is very effective in generating results in these problems, and that the large guide tubes do not significantly impact the code's accuracy. The %RMS pin power differences for each case are depicted in Figure 15 alongside a list of the ordering of the case conditions within the labels designating each assembly.

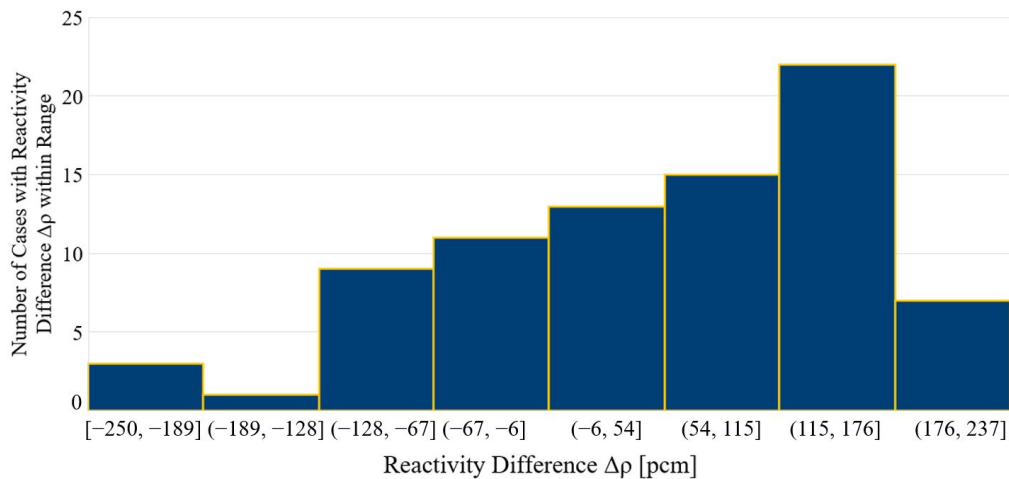


Figure 14. Histogram of reactivity difference for single 2-D assembly problems.

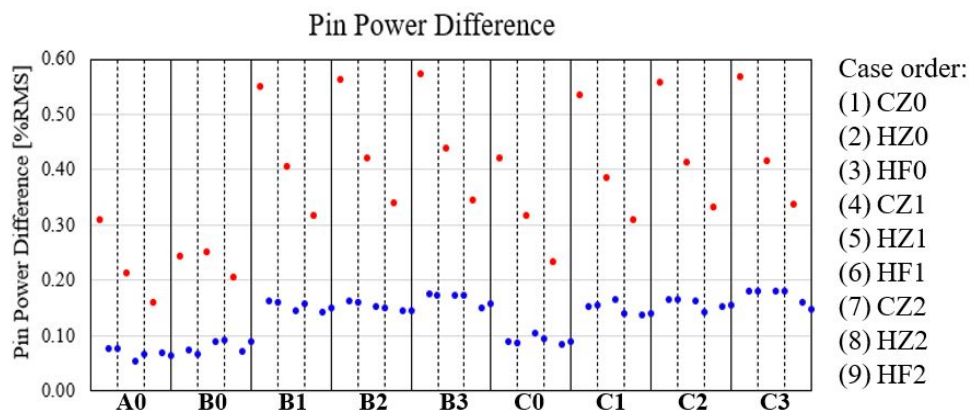


Figure 15. %RMS pin power differences for each 2-D assembly case and list of the case order within each assembly type.

Figure 15 indicates that greatest deviation from the reference solutions was observed in all CZ cases, no matter the boron concentration. These cases are marked in red, and the pin power differences are significantly higher than all other cases for that assembly. All other cases, marked in blue, have lower differences and demonstrate strong agreement between MPACT and McCARD.

Table 3 summarizes the data in Figures 14 and 15 and shows the average k_{inf} difference as well as the average %RMS pin power difference from McCARD for each assembly type.

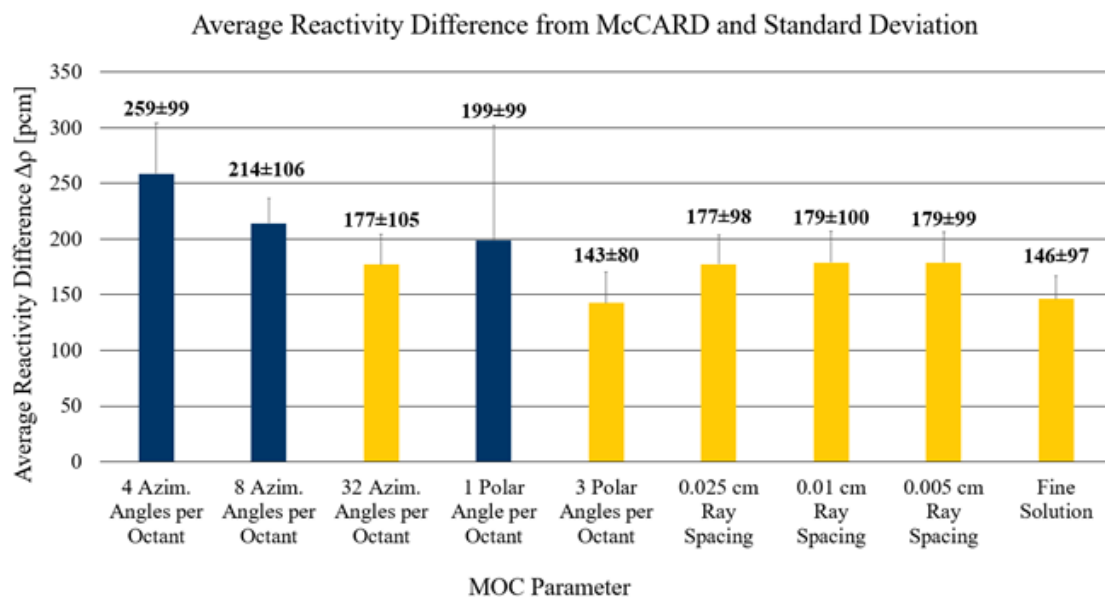
As mentioned in the previous section, reactivity differences are ideally below 200 pcm. For the 2-D assembly problems, eight cases do not meet this goal, and all but two of these have CZ conditions. As such, MPACT shows good agreement with McCARD. Reference [12] also outlines accuracy goals of less than 1.0% RMS difference and less than 1.5% maximum difference for 2-D assembly pin power distributions. Since the highest RMS pin power difference between MPACT and McCARD is 0.57% and the maximum pin power difference is 1.15%, the pin powers calculated by MPACT show excellent agreement with McCARD.

Table 3. Single 2-D assembly results by assembly type.

Assembly Type	Average $k_{inf} \Delta\rho$ [pcm]	Max. $k_{inf} \Delta\rho$ [pcm]	RMS Pin Power Diff. [%]	Max. Pin Power Diff. [%]
A0	83 ± 68	234	0.12	0.69
B0	76 ± 67	225	0.13	0.60
B1	100 ± 64	201	0.24	1.09
B2	103 ± 67	218	0.25	1.15
B3	143 ± 64	250	0.26	1.10
C0	71 ± 74	237	0.17	0.90
C1	83 ± 51	151	0.22	1.06
C2	113 ± 52	182	0.25	1.08
C3	117 ± 57	204	0.26	1.10

3.2.2. MOC Parametric Studies

Nine cases were considered for the 2-D assembly MOC studies: for each of the nine assemblies, MOC parameters were independently changed for the CZ0 case. The results were compared to the McCARD k_{inf} . Just as for the single pin cases, variations included using 4, 8, and 32 azimuthal angles per octant instead of the default 16; 1 and 3 polar angles per octant instead of the default 2; and 0.025 cm, 0.01 cm, and 0.005 cm ray spacing instead of the default 0.05 cm. Figure 16 summarizes the average differences between the k_{inf} generated using each of these parameters and the k_{inf} generated by McCARD as well as the standard deviation.

**Figure 16.** Average difference from MPACT default k_{inf} for 2-D assembly MOC studies.

In Figure 16, blue bars indicate parameters that are less fine than the default values, and maize bars indicate parameters that are finer than the default. For reference, the average difference from McCARD for 2-D assembly CZ0 cases using default MOC parameters was 133 pcm ± 74 pcm.

Significant disagreement ranging from an average of 199 pcm to 259 pcm exists when parameters are made less fine than the default, therefore indicating that using coarser MOC values worsens agreement with McCARD when compared to the default values, as expected. The maximum absolute difference from McCARD is 371 pcm.

However, when MOC parameters are made finer than the default, the average reactivity difference with McCARD is worse than reactivity difference of 133 pcm when using

default parameters in every case; the average difference ranges from 143 pcm to 179 pcm. Even compared to a “fine” solution that had a ray spacing of 0.005 cm, 32 azimuthal angles per octant, and 3 polar angles per octant, the average reactivity difference is 146 pcm, which is 13 pcm higher than the difference when default values are used. A possible explanation is that refining the MOC mesh could be reducing some error cancellation. Specifically, the MPACT cross-section library uses super homogenization (SPH) factors to obtain the best possible agreement, even when different calculation methods are used. The SPH factors are determined by comparing pin cell solutions generated using transport corrected P_0 (TCP₀) scattering with solutions generated using continuous energy Monte Carlo methods. The multigroup resonance integral data are multiplied by these SPH factors. When solving problems using P_2 scattering instead of TCP₀ scattering, as with these benchmark results, the SPH factors become inconsistent, therefore removing some error cancellation and contributing to the significant disagreement observed in Figure 16 above. Hence, given that every alteration to MOC parameters causes worse agreement with McCARD than for default values, default MOC parameters are most appropriate for use in generating benchmark results.

3.2.3. Spatial Mesh Parametric Studies

For the 2-D assembly mesh study, the number of radial subdivisions in the innermost region of the fuel cells was changed from the default of three rings to be one, two, four, or five rings. The gadolinia mesh was also altered from the default value of ten rings to be one, five, or 15 rings. When varying the mesh, ray spacing was 0.01 cm, and the azimuthal and polar angles per octant were left at the default values. The mesh azimuthal angles were left at the default of 8 per octant. The CZ0 case for each assembly type, the same as was used for the MOC studies, was examined for the spatial mesh studies. The average differences between the k_{inf} generated using the various spatial meshes and the k_{inf} calculated by McCARD as well as the standard deviation are shown in Figure 17.

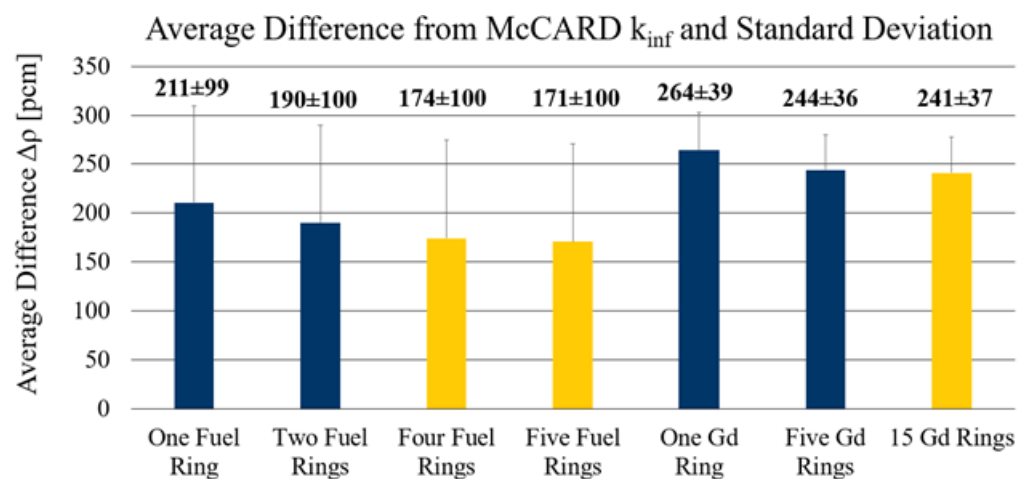


Figure 17. Average difference from MPACT default k_{inf} for 2-D assembly spatial mesh studies.

In Figure 17, blue bars indicate parameters that are less fine than the default values, and yellow bars indicate parameters that are finer than the default. Using coarser spatial meshes than the default results in average reactivity differences from McCARD ranging from 190 pcm to 264 pcm, and using finer spatial meshes results in reactivity differences from 171 pcm to 241 pcm. The maximum absolute difference from McCARD of all the cases was 331 pcm. Like the MOC parametric studies, every alteration of the spatial mesh, including making it finer, has worse average agreement with McCARD than the default mesh, which has an average reactivity difference from McCARD of 133 pcm. This is again likely due to inconsistencies in the SPH factors due to the use of the P_2 scattering method that are accentuated when the mesh is changed.

Every alteration of the gadolinia mesh results in substantially worse agreement with McCARD than is observed for changing the fuel mesh; the finest gadolinia mesh of 15 rings has an average reactivity difference of 241 pcm with McCARD, which is 30 pcm worse than the average reactivity difference for the coarsest fuel spatial mesh of one ring.

As with the MOC parametric study, given that every alteration to the fuel and gad meshes causes agreement with McCARD to worsen, it is most optimal to use the default values of three fuel rings and ten gadolinia rings when generating benchmark results.

3.2.4. Comparison of 2-D Assembly MPACT “Fine” Solution to McCARD

To further examine if default parameters generate appropriate benchmark solutions, 2-D assembly results obtained using the “fine” solution, which has a ray spacing of 0.005 cm, 32 azimuthal angles per octant, and 3 polar angles per octant, were compared to McCARD. These solutions were then compared to how close the default solution was to McCARD. All cases considered were CZ0 cases. Table 4 shows the ρk_{inf} difference and %RMS pin power difference from McCARD for both the solution generated using MPACT’s default parameters and the “fine” solution.

Table 4. Comparison of default and “fine” solution.

Assembly Type	$k_{inf} \Delta\rho$ [pcm]		RMS Pin Power Diff. [%]	
	Default Solution	“Fine” Solution	Default Solution	“Fine” Solution
A0	−76	−56	0.12	0.31
B0	−91	−29	0.12	0.54
B1	−201	−120	0.25	0.50
B2	−218	−220	0.26	0.57
B3	−250	−270	0.27	0.58
C0	−25	−7	0.17	0.42
C1	−106	−167	0.24	0.54
C2	−113	−221	0.26	0.56
C3	−114	−224	0.27	0.57
Average	−133 ± 74	−146 ± 97	0.22	0.51

As seen in Table 4, the average k_{inf} relative difference from McCARD and average RMS pin power differences are both higher for the “fine” solution than using the default parameters. Again, this is likely due to the super homogenization (SPH) factors used by MPACT’s cross-section library that are determined using TCP₀ scattering. Therefore, when solving problems using P₂ scattering instead of TCP₀ scattering, as with these benchmark results, the SPH factors become inconsistent, therefore removing some error cancellation and contributing to increased disagreement from a more refined mesh. Thus, the default parameters are sufficiently optimized and are appropriate to use to generate benchmark problem results.

Figure 18 compares pin power differences of the A0 assembly with CZ0 conditions from McCARD for the default and “fine” solution, and clearly indicates that differences in individual pin powers are quite similar for both solutions. Blue represents minimum difference and maize indicates maximum difference from McCARD.

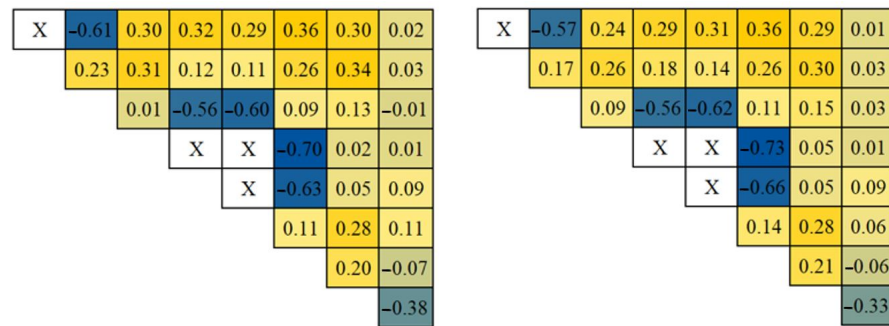


Figure 18. Relative difference [%] in A0 assembly pin powers of MPACT default solution (left) and MPACT “fine” solution (right) from McCARD solution.

3.3. 2-D Core

3.3.1. In-Out Tilt with TCP₀ Scattering

MPACT’s default scattering method is TCP₀. However, the 2-D core radial power distribution results exhibited a noticeable in-out tilt when the default TCP₀ scattering was used. Figure 19 shows the radial assembly powers for the HZ1 case when TCP₀ scattering was used.



Figure 19. In-out tilt in assembly-wise radial power distribution with default TCP₀ scattering in HZ1 case.

In the figure, maize indicates over-estimation of assembly powers, and blue represents under-estimation. The greatest deviations from McCARD are outlined in red. There are clearly defined regions of over- and under-estimation of assembly powers; maize is concentrated in the center regions, with over-estimation ranging from 0.08% to 1.03%. The periphery is dominated by blue, with under-estimation from -0.16% to -0.63%. For the HF1 case, the RMS assembly power difference was 0.45%, and the maximum difference was 1.03%.

To confirm this in-out tilt was caused by TCP₀ scattering, a case with P₂ scattering was performed. Figure 20 shows the radial power distribution for the HZ1 case when the P₂ scattering method is used.

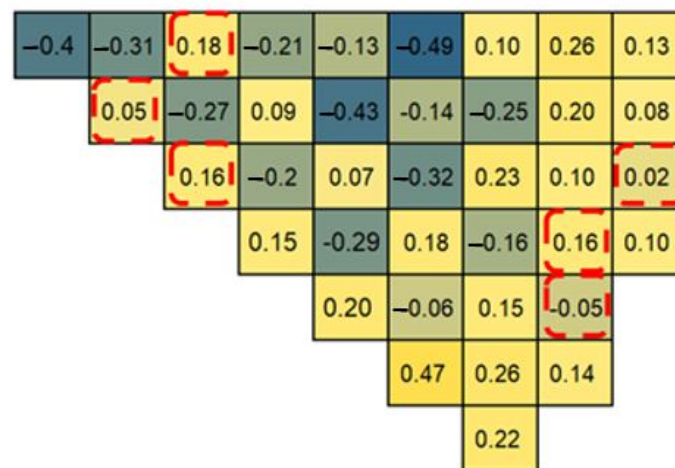


Figure 20. Corrected assembly-wise radial power distribution with P_2 scattering in HZ1 case.

Again, maize represents over-estimation of assembly powers while blue indicates under-estimation. The same color scale is used for Figures 19 and 20 to better compare the two. The power distribution is now much more even, and the regions of over- and under-estimation are not so clear. Additionally, the radial assembly powers show much greater agreement with McCARD; The RMS assembly power difference decreased from 0.45% to 0.23%, and the maximum relative power difference decreased from 1.03% to 0.49%.

The HZ1 case is not unique; every case demonstrated substantially improved agreement when P_2 scattering was used. The specific changes to RMS and maximum assembly power differences when changing from TCP_0 to P_2 scattering are outlined in Table 5.

Table 5. Comparison of RMS and maximum assembly power differences for TCP_0 and P_2 scattering.

Case Condition	RMS Difference [%]		Max. Difference [%]	
	TCP_0	P_2	TCP_0	P_2
CZ0	1.15	0.41	2.54	0.85
HZ0	0.55	0.34	1.31	0.82
HF0	0.51	0.36	1.13	0.67
CZ1	1.24	0.42	3.10	0.85
HZ1	0.45	0.22	1.03	0.48
HF1	0.84	0.39	1.77	1.02
CZ2	1.92	0.47	4.52	0.87
HZ2	1.05	0.18	2.24	0.40
HF2	1.36	0.21	2.53	0.48
Average	1.01	0.33	2.24	0.72

As shown in Table 5, the average RMS assembly power difference decreased from 1.01% to 0.36% and the average maximum assembly power difference decreased from 2.24% to 0.80% when P_2 scattering was used instead of TCP_0 scattering, clearly indicating the P_2 scattering must be used to have acceptable agreement with McCARD. Thus, for all benchmark problems, P_2 scattering was used. P_2 scattering was also tested for the single pin and single 2-D assembly problems, and results were significantly different, so those problems were recalculated using P_2 scattering. All results presented in this report were generated using P_2 scattering.

3.3.2. Results Generated Using P_2 Scattering

As outlined above, when P_2 scattering is used, the 2-D core results generated by MPACT demonstrate strong agreement with the McCARD reference solution. Table 6

summarizes and compares the 2-D core results generated by McCARD and MPACT for each condition.

Table 6. Summary of 2-D core results and comparison between MPACT and McCARD.

Case Condition	McCARD		MPACT	Comparison of MPACT and McCARD			
	k_{eff}	std. [pcm]	k_{eff}	$\Delta\rho$ [pcm]	Assembly Power Diff.		
					RMS [%]	Max. [%]	
CZ0	1.22261	6	1.22040	−148	0.41	0.85	
CZ1	1.03687	7	1.03670	47	0.42	0.85	
CZ2	0.91050	7	0.91098	182	0.47	0.87	
HZ0	1.14693	6	1.14693	0	0.34	0.82	
HZ1	1.02305	6	1.02328	72	0.22	0.48	
HZ2	0.93015	6	0.93044	131	0.18	0.40	
HF0	1.13808	6	1.13768	−31	0.36	0.67	
HF1	1.01523	6	1.01512	40	0.39	1.02	
HF2	0.92316	6	0.92401	99	0.25	0.64	
Average	-	-	-	83 ± 61	0.34	0.73	

The ρ difference for each condition is below 200 pcm for every case, and the overall average ρ difference is 83 pcm \pm 61 pcm. The greatest reactivity difference is for the CZ2 case, which overpredicts k_{eff} by 182 pcm. This maximum difference is below the accuracy goal of 200 pcm difference outlined in [12], indicating good reactivity agreement between MPACT and McCARD.

Regarding the assembly comparisons, MPACT's results agree very well with McCARD; the average RMS assembly power difference is only 0.34%, and the average maximum difference is 0.73%. Reference [12] presents accuracy goals of below 1.5% RMS assembly power differences and below 2.5% maximum assembly power differences. The greatest RMS assembly power difference is 0.47% and the maximum assembly power difference is 1.02%, indicating that MPACT shows good agreement with the power distributions calculated by McCARD.

Generally, the CZ cases have worse reactivity agreement with McCARD than other case conditions. There are several possible explanations for this. Specifically, it is possible that the hydrogen scattering matrix used by either McCARD or MPACT is incorrect; temperature dependence is not accounted for in the scattering kernel for hydrogen, which results in inaccuracies in the scattering matrix. Since hydrogen plays such an important role in light water reactors, small changes in the scattering kernel can substantially impact results [13]. To determine if the scattering matrix used by McCARD caused these issues, single fuel pin and 2-D assembly results generated by MPACT using CZ conditions were compared to those generated by the Monte Carlo code Serpent [14]. The disagreement in pin power and reactivity between MPACT and Serpent was comparable to the disagreement between MPACT and McCARD, indicating that if the cold zero bias is caused by an incorrect scattering matrix, it is the scattering matrix used by MPACT and not McCARD. It was also suggested that there may be a spatial discretization error in which there are too few rings in the mesh for the moderator. However, this was investigated, and refining the moderator mesh did not resolve the cold zero bias.

3.4. 3-D Core

3-D Core Results

Table 7 summarizes and compares the 3-D core results from McCARD and MPACT for each condition. The standard deviation for all Monte Carlo cases is 4 pcm. P_2 scattering was again used because similar to the 2-D results, TCP_0 scattering caused in-out power tilt.

Generally, the results agree well with the McCARD reference solution. The k_{eff} difference is below 150 pcm in every case except for CZ0 and HF0, in which case it

was -156 pcm and 168 pcm, respectively. All reactivity differences are below 200 pcm, indicating good reactivity agreement between MPACT and McCARD.

Table 7. Summary of 3-D core results and comparison between MPACT and McCARD.

Case Condition	McCARD	MPACT	Comparison of MPACT and McCARD				
	k_{eff}	k_{eff}	$\Delta\rho$ [pcm]	Assembly Power Diff.		Axial Power Diff.	
				RMS [%]	Max [%]	RMS [%]	Max [%]
CZ0	1.21765	1.21534	-156	0.46	1.07	0.55	1.95
CZ1	1.03406	1.03448	39	0.46	0.98	1.65	3.04
CZ2	0.90907	0.91046	168	1.17	2.57	0.77	1.39
HZ0	1.13942	1.13938	-3	0.48	1.27	1.38	2.53
HZ1	1.01760	1.01829	67	0.38	0.79	0.88	1.65
HZ2	0.92594	0.92709	134	0.22	0.57	0.34	0.93
HF0	1.13061	1.13013	-38	0.56	1.26	1.18	2.81
HF1	1.00973	1.01013	39	0.32	0.72	0.58	1.91
HF2	0.91899	0.91979	94	0.30	1.03	0.77	1.39
Average	-	-	82 ± 59	0.49	1.14	0.90	1.96

Additionally, all RMS assembly power differences are below 0.56% with the exception of the HF0 case, which had an RMS assembly power difference 1.17% , respectively. Axial power differences are slightly larger; the largest RMS axial power difference is 1.65% , and the maximum axial power difference is 3.04% . Reference [12] gives an accuracy goal of 2.0% RMS difference and 3.0% maximum difference for both radial and axial power distributions. The radial RMS and maximum assembly power differences are all below these goals, indicating good agreement of radial power distributions between MPACT and McCARD. Regarding axial power differences, the RMS differences are all below 2.0% , but the maximum difference of 3.04% exceeds the accuracy goal of 3.0% , albeit slightly. However, all other maximum axial power differences are below 3.0% , with most falling below 2.0% , indicating acceptable agreement between the axial powers calculated by MPACT and those found by McCARD.

For each boron concentration, the temperature condition with the greatest overall deviation from McCARD is the CZ case, which is consistent with the results from previous problems. As noted above, this may be caused by an incorrect hydrogen scattering matrix being used by MPACT.

Figure 21 depicts the RMS axial power differences for each case.

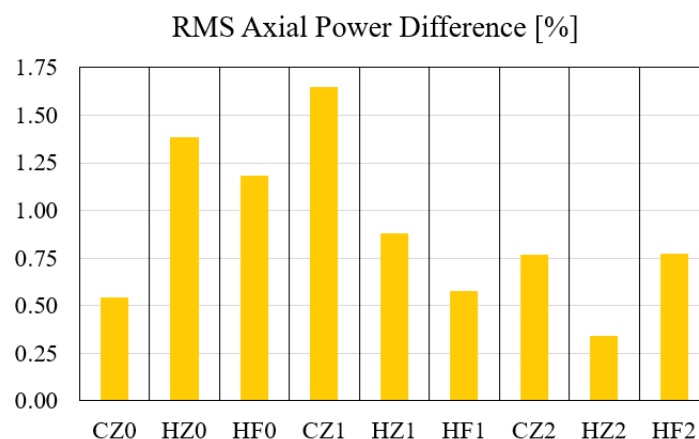


Figure 21. RMS axial power differences for each case condition.

Figure 21 indicates that generally, axial power agreement increases as boron concentration increases.

Figures 22 and 23 show the axial power and relative difference from McCARD for the CZ1 and HZ2 cases, respectively. The disagreement with McCARD is much greater for the CZ1 case, as indicated by the greater relative difference values, which are represented by the blue line in each figure, in Figure 22 when compared to Figure 23.

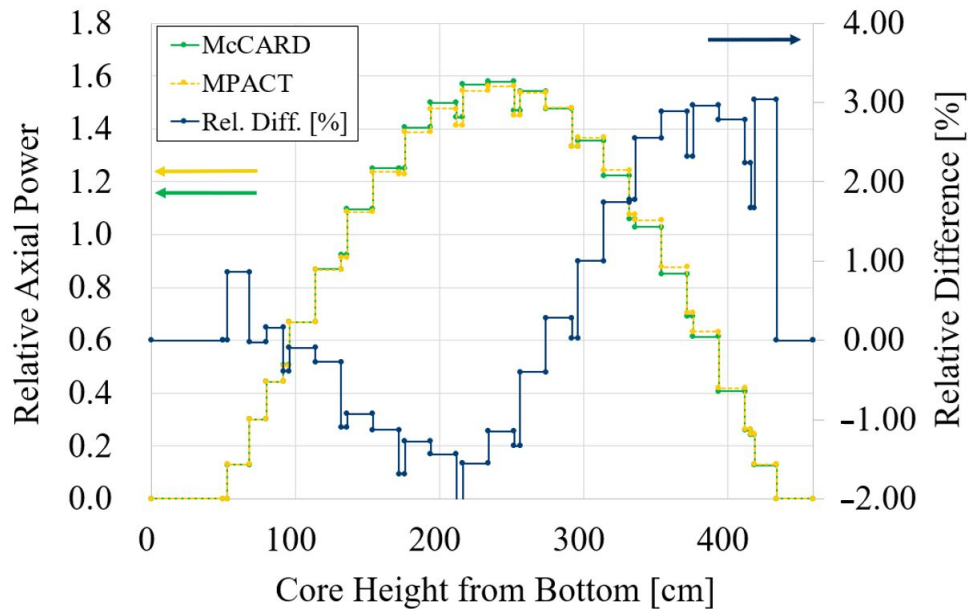


Figure 22. Axial power and relative difference from McCARD for CZ1 case.

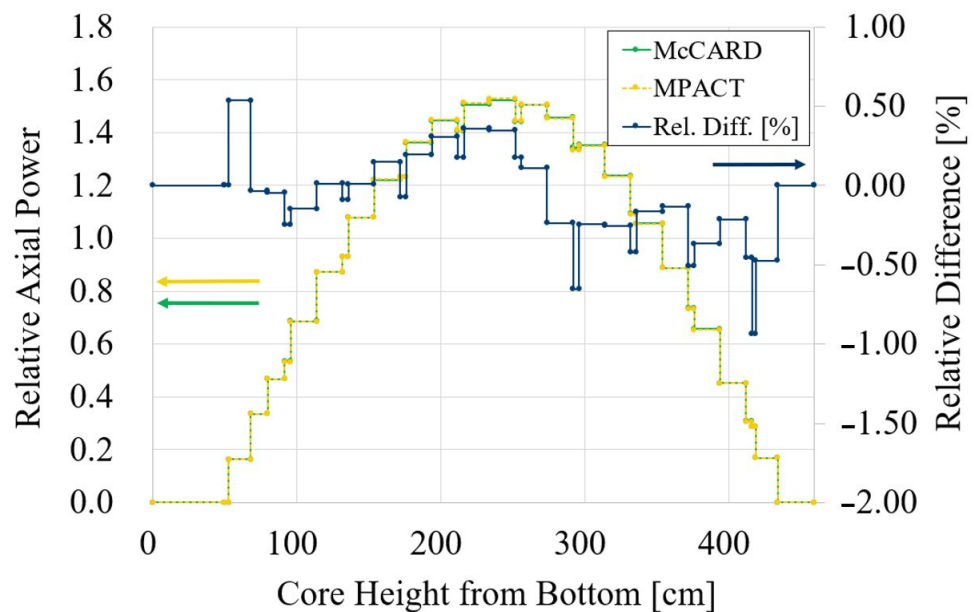


Figure 23. Axial power and relative difference from McCARD for HZ2 case.

3.5. Control Rod Worth

3.5.1. Control Rod Assembly Configuration and Problem Setup

In the APR1400, there are seven control rod banks. Five banks are regulating groups, and are labeled 1, 2, 3, 4, and 5, and two banks are shutdown groups labeled A and B. Banks A, B, 1, and some of bank 2 are 12-fingers assemblies, and some of bank 2 as well as banks 3, 4, and 5 are 4-fingers assemblies.

All cases used HZ0 conditions. There were seven cases studied for the control rod worth problems, plus the all rods out (ARO) case, which is the HZ0 case from the 3-D core problems. For each case, all seven banks were inserted one at a time, following the order 5–4–3–2–1–B–A. There was no withdrawal of previously considered banks.

3.5.2. Worth Equation

The values used to compare results generated by MPACT and McCARD were the accumulated worth and the group worth.

Worth was calculated using Equation (1)

$$worth = \frac{1}{k_i} - \frac{1}{k_{i-1}} \quad (1)$$

where i is the case index. Since the insertion order follows 5–4–3–2–1–B–A, $i = 0$ corresponds to the ARO case, which has a worth of 0 pcm, $i = 1$ corresponds to just bank 5 inserted, $i = 2$ corresponds to banks 5 and 4 inserted, etc.

3.5.3. Accumulated Worth

Accumulated worth is the sum of the worth for all banks inserted thus far and was calculated using the relationship in Equation (2).

$$\text{Accumulated worth} = \sum_{i=1}^n (worth_i) \quad (2)$$

where n is the number of inserted banks.

3.5.4. Group Worth

Group worth refers to the difference in accumulated worth due to inserting a specific control rod bank and was determined using the formula in Equation (3).

$$\text{Group worth for case } i = \sum_{i=1}^n (worth_i) - \sum_{i=1}^{n-1} (worth_i) \quad (3)$$

For example, Group 2 worth = $\sum_{i=1}^4 (worth)_i - \sum_{i=1}^3 (worth)_i$.

3.5.5. Control Rod Worth Results

Table 8 summarizes the control rod worth results and compares the results from MPACT and McCARD.

Table 8. Summary of control rod worth results and comparison between MPACT and McCARD.

Bank(s) Inserted	McCARD		MPACT		Comparison of MPACT and McCARD			
	Group Worth [pcm]	Accum. Worth [pcm]	Group Worth [pcm]	Accum. Worth [pcm]	Group Diff. [%]	Accum. Diff. [%]	Assembly Power Diff.	
							RMS [%]	Max [%]
ARO	0.0	0.0	0.0	0.0	-	-	-	-
5	369.0	369.0	366.7	366.7	−0.6	−0.6	0.21	0.37
5-4	322.7	691.7	323.2	689.9	0.1	−0.3	0.31	0.90
5-4-3	999.4	1691.1	1001.3	1691.2	0.2	0.0	0.37	0.66
5-4-3-2	1041.9	2733.0	1042.7	2733.9	0.1	0.0	0.29	0.67
5-4-3-2-1	2010.0	4743.0	2005.4	4739.3	−0.2	−0.1	0.62	1.44
5-4-3-2-1-B	4142.2	8885.2	4163.1	8902.3	0.5	0.2	0.71	1.86
5-4-3-2-1-B-A	7234.0	16,119.2	7203.4	16,105.7	−0.4	−0.1	0.35	0.84

Again, there is substantial agreement between MPACT and McCARD. All group and accumulated differences are at or below 0.6%. Reference [15] outlines an accuracy goal of below 5% difference in group and accumulated rod bank worths. Since the maximum difference in group and accumulated worths is only 0.6%, MPACT's control rod worths show excellent agreement with McCARD. The greatest deviations from the group and accumulated control rod worths generated by McCARD occur when banks 5 and B are inserted.

Additionally, there is excellent agreement in the assembly powers; all RMS assembly power differences are below 0.71%, and the maximum difference is 1.86%. Assembly power agreement is significantly worse than for all other cases when banks 1 and B are inserted. Similar results were noted for DeCART, and assembly power differences between nTRACER and McCARD were not reported. When examining the radial power distribution, it appears that the greatest differences are in the center of the core, with agreement much stronger on the periphery. Since more absorbers have been inserted, power peaks are pushed away and the power shape becomes very complicated, resulting in errors in calculations when using transport codes as opposed to Monte Carlo codes. When these cases are excluded, the RMS assembly power differences are at or below 0.37%, and the maximum difference is only 0.90%.

3.6. 3-D Core Hot Full Power Depletion

3.6.1. 3-D Core Depletion Results

The depletion was done using a 3-D core model with 100% rated power, a coolant inlet temperature of 563.75 K, and critical boron concentration search at each burnup step. In the input, the axial geometry was adjusted slightly; the height of the upper axial reflector decreased from 25 cm to 5 cm.

No McCARD reference solution was provided for the 3-D core depletion problem, so MPACT results were compared to results generated by other benchmark participants using DeCART and nTRACER [16]. The result from all three codes are shown in Figure 24.

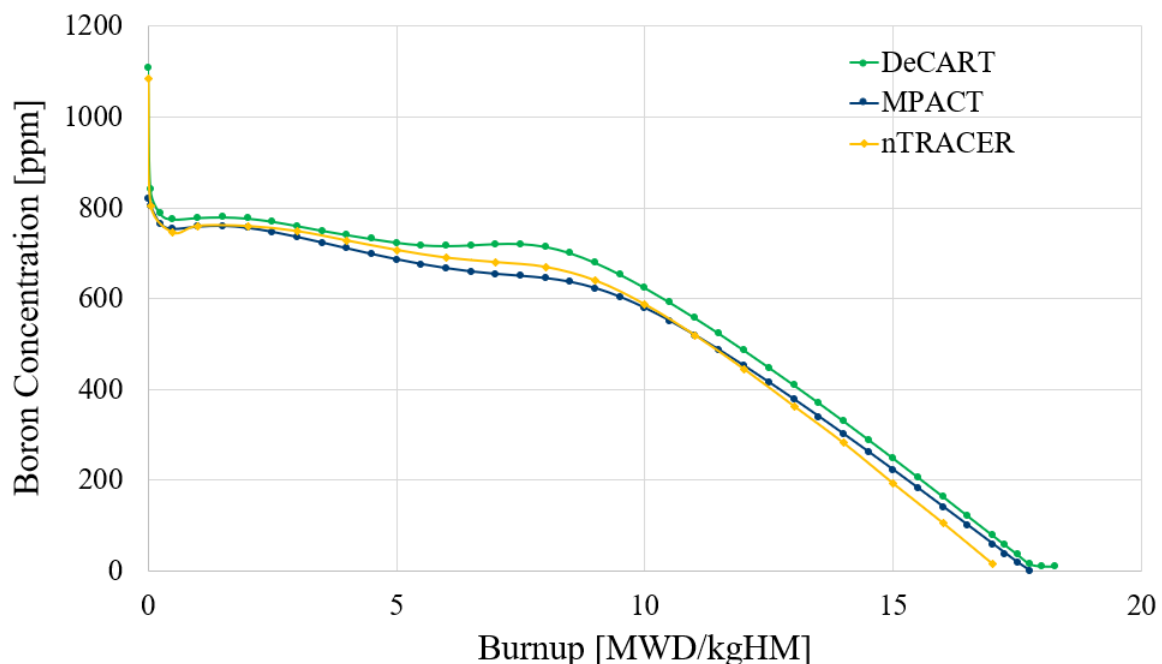


Figure 24. 3-D core depletion results in comparison to solutions generated by other benchmark participants.

Figure 24 shows that the boron concentration calculated by MPACT reaches 0 ppm by 17.75 MWD/kgHM. Overall, MPACT's results are more similar to nTRACER's than DeCART's. MPACT's boron concentration is almost identical to nTRACER's for burnup

of 0.05 MWD/kgHM to 2.5 MWD/kgHM. From 2.5 MWD/kgHM to 10 MWD/kgHM, MPACT reports the lowest boron concentration of the three codes. From 12 MWD/kgHM until the maximum burnup of about 18 MWD/kgHM considered, MPACT's boron concentration is between nTRACER's and DeCART's, but MPACT's boron concentration is closer to DeCART's than nTRACER's from 14.5 MWD/kgHM to 18 MWD/kgHM. For each burnup level, the boron concentration calculated by MPACT is lower than that calculated by DeCART. Table 9 provides more detail about the different boron concentrations by presenting the boron concentrations calculated by MPACT, DeCART, and nTRACER for different burnups and the difference of DeCART and nTRACER from MPACT.

Table 9. MPACT, DeCART, and nTRACER boron concentrations for different burnups.

Burnup [MWD/kgHM]	MPACT	DeCART		nTRACER	
	Boron Conc. [ppm]	Boron Conc. [ppm]	Diff. from MPACT	Boron Conc. [ppm]	Diff. from MPACT
0	1083.50	1107.56	−24.06	1085.05	−1.55
0.05	804.13	840.73	−36.60	804.85	−0.72
0.5	753.12	774.49	−21.37	745.33	7.79
1	758.04	777.70	−19.66	760.32	−2.28
2	755.54	776.44	−20.90	759.79	−4.25
3	735.58	759.99	−24.41	748.58	−13.00
4	710.47	740.27	−29.80	727.85	−17.38
5	686.32	723.33	−37.01	707.17	−20.85
6	666.70	715.86	−49.17	690.03	−23.33
7	654.05	720.33	−66.28	680.34	−26.29
8	644.79	714.19	−69.40	669.75	−24.96
9	622.80	679.05	−56.25	639.88	−17.08
10	579.05	623.64	−44.59	586.93	−7.88
11	519.56	557.81	−38.25	519.66	0.10
12	451.16	485.78	−34.62	444.04	7.12
13	377.69	409.59	−31.60	362.94	14.75
14	301.01	330.27	−29.26	281.73	19.28
15	221.85	248.19	−26.34	192.45	29.40
16	140.83	164.13	−23.30	105.68	35.15
17	58.76	78.57	−19.81	15.43	43.33
18	0.00	10.00	−10.00	0.00	0.00
Average	-	-	34 ± 16	-	15 ± 20

The average boron concentration difference from MPACT is only 15 ppm for nTRACER and 32 ppm for DeCART, indicating that MPACT's calculations are slightly closer to nTRACER's, as noted above. The largest differences from MPACT for DeCART occur at 8 MWD/kgHM, and this appears to be around the time that the gadolinia is depleted. The prediction of the burnout of gadolinium is well understood to be challenging, so the peak difference being here is not surprising. Additional investigations should be performed to try to identify and confirm the root cause of this peak difference. For MPACT and nTRACER, the largest difference occurs near the end of cycle. When comparing the two critical boron concentration curves in Figure 24, it appears that the rate of fuel consumption is different between the two codes, as indicated by the differing slopes after 10 MWD/kgHM. This suggests the κ values, or energy release per fission used for flux normalization in depletion, are different. A suggested follow up study would be to have the three codes perform the cycle depletion calculation with the same κ . Additionally, the differences in the hot full power depletion results are also likely the result of differences in the thermal hydraulics models and parameters used by MPACT, DeCART, and nTRACER. Specifically, all three codes generated results using a simplified thermal hydraulics models that has 1-D closed channel convection and 1-D radial conduction. However, nTRACER and DeCART solved

for convection on a pin-wise basis whereas MPACT used a quarter assembly flow channel. This along with differences in thermophysical property correlations and steam tables could contribute to the observed differences in the depletion results. Although the potential differences in the κ value used as well as the method of solving for pin-wise convection may seem to be subtle differences between the codes, these differences clearly have substantial impacts on the results of calculations.

3.6.2. Burnup Interval Sensitivity for Gadolinia

The burnup interval used for the depletion was 14 EFPD, which equals approximately 0.54 MWD/kgHM. There were concerns that this interval may be too large because gadolinia has a large absorption cross-section, so the reaction rate of gadolinia changes dramatically over time. As such, a smaller interval may be necessary to obtain accurate results. To test this, burnup intervals of 0.5 MWD/kgHM and 0.25 MWD/kgHM burnup interval for 2D assembly depletion were tested, and the calculated k_{inf} values were compared. The results are shown in Figure 25.

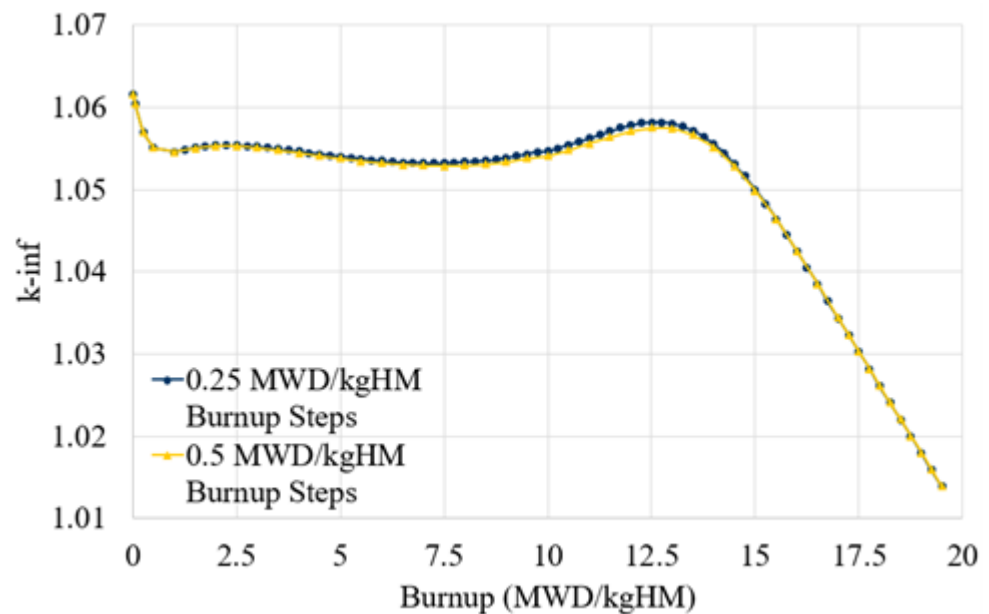


Figure 25. k_{inf} calculated using burnup intervals of 0.5 MWD/kgHM and 0.25 MWD/kgHM.

In Figure 25, the k_{inf} calculated using the different burnup steps is nearly indistinguishable for every level of burnup. The average ρ difference is 21 pcm, and the maximum ρ difference is only 63 pcm. Given the strong agreement between the k_{inf} values calculated using both burnup intervals, it was determined that the burnup interval of 0.54 MWD/kgHM, or 14 EFPD, used for the 3-D core depletion problem was acceptable.

4. Methodology

4.1. Methodologies in MPACT

MPACT is a 3-D full-core neutron transport code capable of calculating subpin level power distribution [1]. Calculations are based on multigroup Boltzmann neutron transport equation. MPACT is capable of treating explicit geometrical configuration of reactor core components. The multigroup cross-section data are pre-generated with resonance parameters, and the resonance self-shielding calculation is performed on-the-fly to calculate problem-dependent self-shielded cross-sections. For a practical 3-D full-core transport calculation, MPACT uses a 2-D/1-D method that combines 2-D method of characteristics (MOC) and 1-D nodal P_3 method. The 2-D radial and 1-D axial solutions are coupled through transverse leakages. The optimally diffusive Coarse Mesh Finite Difference (od-CMFD) method is to accelerate the convergence rate of the transport solution [17]. MPACT

is coupled with ORIGEN to calculate the burnable material compositions as the material is irradiated [18].

In this paper, McCARD is used as reference. Unlike MPACT, McCARD is continuous energy Monte Carlo code [7]. McCARD uses continuous cross-section data in the simulation to represent the neutron behavior as it is. The mesh discretization error can be ignored with McCARD since the Monte Carlo method is used in the neutron transport calculation. Since McCARD (and other Monte Carlo codes) has better accuracy in terms of above two points, the Monte Carlo code is used as a reference for deterministic code solution. However, since a solution from the Monte Carlo method contains a statistical error, it is necessary to use sufficient neutron histories to obtain a reliable solution. In general, it is difficult to calculate accurate pin power distribution for a large size problem such as reactor core.

4.2. Modeling Parameters

Results were generated using MPACT's 2-D transport solver. All cases used the 51-group cross-section library with ENDF/B-VII.1 data and default meshing parameters. For pin cells, the default MOC flat source discretization was used. In fuel cells, the default flat source discretization creates 3 equal-area radial subdivisions in the fuel and one ring each in the fuel-clad gap, zircaloy cladding, and moderator. The guide tube pin cell has 3 radial subdivisions in the interior moderator and radial subdivision each in the cladding and external moderator. In the gadolinia burnable absorbers, there are 10 radial subdivisions in the fuel and 1 radial subdivision in all other regions. Each radial subdivision in all cell types has 8 azimuthal divisions. The flat source characteristics solver was used instead of the linear source characteristics solver because the linear source solver is still undergoing validation. For the MOC discretization, the Chebyshev-Yamamoto quadrature type was used with a ray spacing of 0.05 cm, 16 azimuthal angles per octant, and 2 polar angles per octant. The P_2 scattering method was used for all problems.

All materials were defined based on the isotope number densities provided in the benchmark specifications [6]. However, there were some isotopes missing from MPACT's cross-section library for which substitutions were necessary. Specifically, for silicon, carbon, and molybdenum, the benchmark specified number densities for individual stable isotopes of these elements, but MPACT's cross-section library does not have entries for the individual isotopes. Rather, the cross-sections for natural silicon, natural carbon, and natural molybdenum were used instead because the number densities of various isotopes in the natural elements are the same as the individual isotopes specified in the benchmark.

4.3. Relevant Equations for Analysis

4.3.1. Reactivity Differences

All reactivity differences are reported in terms of $\Delta\rho$, where $\Delta\rho$ is defined in Equation (4).

$$\Delta\rho = \frac{1}{k_{\text{McCARD}}} - \frac{1}{k_{\text{MPACT}}}. \quad (4)$$

When results from multiple cases are combined, the arithmetic mean of $\Delta\rho$ is used.

4.3.2. Pin and Assembly Power Comparisons

Pin and assembly power comparisons are usually reported in terms of the relative root-mean-square (%RMS) difference. The relative difference, ϵ , between MPACT and McCARD is defined in Equation (5).

$$\epsilon = \frac{\text{Power}_{\text{MPACT}} - \text{Power}_{\text{McCARD}}}{\text{Power}_{\text{McCARD}}}. \quad (5)$$

Using this result, the %RMS different is defined in Equation (6).

$$\%RMS = \sqrt{\frac{\sum_{i=1}^n (\epsilon)_i^2}{n}} \quad (6)$$

where i is the pin or assembly index, and n is the total number of pins or assemblies considered. For maximum pin and assembly power differences, the relative maximum difference of all pins or assemblies considered, calculated using the above relative difference formula, is used.

5. Conclusions

Overall, MPACT shows excellent agreement compared to the Monte Carlo reference solution generated by McCARD. MOC and spatial mesh parametric studies indicate that default meshing parameters and options yield results comparable to finely meshed cases, so default parameters are appropriate for use in generating results for benchmark problems. MPACT effectively predicts reactivity for several problem types and conditions. The highest errors exist for CZ conditions, but excluding these cases, the ρ reactivity difference is consistently below 100 pcm. Additionally, for the single fuel pin problems, the greatest disagreement existed for the lowest fuel enrichment of 1.71 wt.% UO₂, indicating possible enrichment bias in MPACT's cross-section library. Moreover, there is strong agreement of the radial and axial power distributions. The use of P₂ scattering corrected the in-out radial power tilt caused using the default TCP₀ scattering method. With P₂ scattering, all RMS pin and assembly power are differences below 1%, and all RMS axial power differences are below 1.65%. These results are comparable to previous results from the VERA progression problems benchmark [1,19] and below the accuracy goals outlined in [12,15]. Regarding the hot full power 3-D core depletion, there was some variation in the critical boron concentration calculated by MPACT compared to nTRACER and DeCART. MPACT's boron concentration is closer to nTRACER's concentration than DeCART's for each burnup level.

Despite the good validation base of MPACT, nTracer, and DeCART as well as the similarities in methodology, the differences in results can vary beyond previously stated accuracy goals. This is particularly evident for the operational conditions where obtaining a better Monte Carlo reference solution is still challenging. This observation suggests that high-fidelity whole-core reactor analysis tools should only be considered predictive once validated. The corollary of this is that this consideration does not necessarily apply to new reactor types that do not have data for validation. At first, this conclusion may seem to undermine the whole effort of advanced reactor simulation, but the authors wish to suggest that this conclusion is not necessarily a remark on the methodologies of these codes since they have been validated for other systems. Rather, we suggest it is more a remark on variation of the modeling choices. Here, we consider the differences of the MPACT, nTracer, and DeCART simulations of the APR1400 cycle depletion as a result of modeling choices, although one could argue they are methodological. Consequently, in the field of reactor analysis, having validated models is just as important as having validated codes.

6. Future Work

The results of this research generate questions that will be investigated in future work. Specifically, for the single fuel pin studies, there is greater agreement for pin cells with higher fuel enrichments, so this enrichment bias, which may be due to bias in MPACT's cross-section library, will be investigated. Additionally, for each problem, the highest errors existed for cases with cold zero power conditions. This can possibly be explained by an incorrect hydrogen scattering matrix used by MPACT. This possibility will be investigated further. Finally, there were significant differences between MPACT, nTRACER, and DeCART in the hot full power 3-D depletion problem. The causes of these differences will be investigated.

Author Contributions: Conceptualization, B.K.; Data curation, K.E.B.; Formal analysis, K.E.B.; Funding acquisition, B.K.; Investigation, K.E.B. and J.K.; Methodology, K.E.B. and S.C.; Project administration, K.E.B.; Resources, B.K.; Software, K.E.B., S.C. and B.K.; Supervision, B.K.; Validation, K.E.B., S.C. and B.K.; Visualization, K.E.B.; Writing—original draft, K.E.B.; Writing—review and editing, K.E.B., S.C., J.K. and B.K. All authors have read and agreed to the published version of the manuscript.

Funding: This research was supported by the Consortium for the Simulation of Light Water Reactors, an Energy Innovation Hub for Modeling and Simulation of Nuclear Reactors under U.S. Department of Energy Contract No. DE-AC05-00OR22725. This research also made use of the resources at the High-Performance Computing Center at Idaho National Laboratory, that is also supported by the Office of Nuclear Energy of the U.S. Department of Energy and the Nuclear Science User Facilities under Contract No. DE-AC07-05ID14517.

Institutional Review Board Statement: Not applicable.

Informed Consent Statement: Not applicable.

Data Availability Statement: Data can be made available upon making a request to the corresponding author.

Acknowledgments: This work was performed under the I-NERI in collaboration with ORNL, ANL, North Carolina State University, KAERI, Seoul National University and Ulsan National Institute of Science and Technology. The authors also wish to express their personal gratitude to Jin-Young Cho, Han-gyu Joo, and Seungsu Yuk for their helpful contributions in the analysis of this benchmark.

Conflicts of Interest: The authors declare no conflict of interest. The funders had no role in the design of the study; in the collection, analyses, or interpretation of data; in the writing of the manuscript, or in the decision to publish the results.

Abbreviations

The following abbreviations are used in this manuscript:

APR1400	Advanced Power Reactor 1400 MWe
ANL	Argonne National Laboratory
CZ	Cold zero
DeCART	Deterministic Core Analysis based on Ray Tracing
HF	Hot full
HZ	Hot zero
I-NERI	International Nuclear Energy Research Initiative
KAERI	Korea Atomic Energy Research Institute
MOC	Method of Characteristics
MPACT	Michigan PArallel Characteristics Transport
NURAM	Nuclear Reactor Analysis and Methods
ORNL	Oak Ridge National Laboratory
%RMS	Relative Root Mean Square
SPH	Super homogenization
UM	University of Michigan

References

1. Downar, T.; Kochunas, B.; Collins, B. *MPACT Verification and Validation Manual (Rev 4)*; Technical Report CASL-U-2018-1641-000; Consortium for Advanced Simulation of Light Water Reactors: Oak Ridge, TN, USA, 2018.
2. Collins, B.; Godfrey, A.T.; Stimpson, S.; Palmtag, S. Simulation of the BEAVRS Benchmark using VERA. In Proceedings of the International Conference Mathematics and Computational Methods Applied to Nuclear Science and Engineering, Jeju, Korea, 16–20 April 2017.
3. Godfrey, A.T.; Collins, B.; Kim, K.S.; Montgomery, R.; Powers, J.J.; Salko, R.K.; Stimpson, S.; Wieselquist, W.A.; Clarno, K.T.; Gehin, J.C.; et al. *VERA Benchmarking Results for Watts Bar Nuclear Plant Unit 1 Cycles 1–12*; Technical Report CASL-U-2015-0206-000; Consortium for Advanced Simulation of Light Water Reactors: Oak Ridge, TN, USA, 2018.
4. Liu, Y.; Vaughn, K.; Kochunas, B.; Downar, T.J. Validation of Pin-Resolved Reaction Rates, Kinetics Parameters, and Linear Source MOC in MPACT. *Nucl. Sci. Eng.* **2021**, *195*, 50–68. [[CrossRef](#)]

5. *Fiscal Year 2013 Annual Report*; Technical Report I-NERI-2013; U.S. Department of Energy Office for Nuclear Energy: Washington, DC, USA, 2013.
6. Yuk, S. *APR1400 Reactor Core Benchmark Problem Book*; Technical Report RPL-INERICA-004; Korea Atomic Energy Research Institute: Daejeon, Korea, 2019.
7. Shim, H.J.; Han, B.S.; Jung, J.S.; Park, H.J.; Kim, C.H. McCARD: Monte Carlo Code for Advanced Reactor Design and Analysis. *Nucl. Eng. Technol.* **2012**, *44*, 161–176. [[CrossRef](#)]
8. *MPACT Theory Manual Version 2.2.0*; Technical Report CASL-U-2016-1107-000; Consortium for Advanced Simulation of Light Water Reactors: Oak Ridge, TN, USA, 2016.
9. Joo, H.G.; Cho, J.Y.; Kim, K.S.; Lee, C.C.; Zee, S.Q. Methods and Performance of a Three-Dimensional Whole-Core Transport Code DeCART. In Proceedings of the PHYSOR, Chicago, IL, USA, 25–29 April 2004; pp. 134–156.
10. Hong, H.; Joo, H. Analysis of the APR1400 PWR Initial Core with the nTRACER Direct Whole Core Calculation Code and the McCARD Monte Carlo Code. In Proceedings of the Transaction of the KNS Spring Meeting, Jeju, Korea, 17–19 May 2017.
11. Yuk, S. *DeCART Solutions of APR1400 Reactor Core Benchmark Problems*; Technical Report KAERI/TR-7826/2019; Korea Atomic Energy Research Institute: Daejeon, Korea, 2019.
12. Kim, K.S.; Clarno, K.T.; Gentry, C.; Wiarda, D.; Williams, M.L.; Kochunas, B.; Liu, Y.; Palmtag, S.; Godfrey, A.T. *Development of the V4.2m5 and V5.0m0 Multigroup Cross Section Libraries for MPACT for PWR and BWR*; Technical Report CASL-U-2017-1280-000; Consortium for Advanced Simulation of Light Water Reactors: Oak Ridge, TN, USA, 2017.
13. Park, H. Resonance Treatment Innovations for Efficiency and Accuracy Enhancement in Direct Whole Core Calculations of Water-Cooled Power Reactors. Ph.D. Thesis, Seoul National University, Seoul, Korea, 2018.
14. Leppänen, J.; Pusa, M.; Viitanen, T.; Valtavirta, V.; Kaltiaisenaho, T. The Serpent Monte Carlo code: Status, development and applications in 2013. *Ann. Nucl. Energy* **2014**, *82*, 142–150. [[CrossRef](#)]
15. Smith, K.; Forget B. Challenges in the Development of High-Fidelity LWR Core Neutronics Tools. In Proceedings of the International Conference on Mathematics and Computational Methods Applied to Nuclear Science and Engineering, Sun Valley, ID, USA, 5–9 May 2013.
16. Kang, J.; Joo, H.G. nTRACER Solutions of APR1400 Benchmark and Fast Reactor Analysis Status. In Proceedings of the 3rd I-NERI Progress Meeting, Atlanta, Georgia, 29 March–3 April 2019.
17. Zhu, A.; Jarrett, M.; Xu, Y.; Kochunas, B.; Larsen, E.; Downar, T. An Optimally Diffusive Coarse Mesh Finite Difference Method to Accelerate Neutron Transport Calculations. *Ann. Nucl. Energy* **2016**, *95*, 116–124. [[CrossRef](#)]
18. Gauld, I.C.; Radulescu, G.; Ilas, G.; Murphy, M.D.; Williams, M.L.; Wiarda, D. Isotopic Depletion and Decay Methods and Analysis Capabilities in SCALE. *Nucl. Technol.* **2011**, *174*, 169. [[CrossRef](#)]
19. Godfrey, A.T. *MPACT Testing and Benchmarking Results*; Technical Report CASL-U2014-0045-000; Consortium for Advanced Simulation of Light Water Reactors: Oak Ridge, TN, USA, 2014.